P-wave ray (group) velocities in a weak-anisotropy approximation

Véronique Farra [1] and Ivan Pšenčík [2]

[1]Institut de Physique du Globe de Paris, Sorbonne Paris Cité, UMR 7154 CNRS, France. E-mail: farra@ipgp.fr
[2]Institute of Geophysics, Acad. Sci. of Czech Republic, Boční II, 141 31 Praha 4, Czech Republic. E-mail: ip@ig.cas.cz

Abstract

We test accuracy of the weak-anisotropy approximation of the ray (group)-velocity formulae. The formulae of varying accuracy are applicable to anisotropy of arbitrary symmetry and orientation. They provide the square of the magnitude of the ray velocity as a function of a ray vector, i.e., a unit vector pointing in the direction of the ray-velocity vector. The ray velocity (phase velocity too) is expressed in terms of three elements of the rotated Christoffel matrix, which depend linearly on the parameters specifying the medium. The less accurate formulae are fully independent of the choice of a reference isotropic medium, the most accurate formula depends only slightly on the ratio of S- and P-wave velocities of the reference medium. We show that the accuracy of the formulae is close to the accuracy of the so-called anelliptic approximations, very accurate approximations based on perturbation of elliptical anisotropy.

Introduction

There is an increasing demand for the analytical expressions for the ray (group) velocity in anisotropic media of various symmetries (Song and Every, 2000; Daley and Krebes, 2004; Fomel, 2004; Sripanich and Fomel, 2014; Hao and Stovas, 2015). Such expressions are required, for example, in moveout expressions (Tsvankin, 2001; Tsvankin and Grechka, 2011), in prestack time migration (Alkhalifah, 2000b) or in finite-difference computations of traveltimes (Fomel, 2004). The task is often complicated by an additional request for expressions providing the ray velocity as a function of the ray angle (Alkhalifah, 2000b; Fomel, 2004; Hao and Stovas, 2015). The above references describe, in detail, history and give overviews of various approaches to solving this problem. For its solution, we use an alternative approach based on the weak-anisotropy approximation. Although it is designed for weakly anisotropic media, it yields, even for moderately anisotropic media, results of accuracy comparable with approaches proposed in the above references.

Presented expressions are obtained by expansions of the exact ray-velocity formula with respect to weak-anisotropy (WA) parameters. WA parameters represent an alternative parameterization of the medium to the commonly used elastic moduli in the Voigt notation. They are similar to Thomsen-type parameterization. They can, however, be

Seismic Waves in Complex 3–D Structures, **25** (2015), 157–175 (ISSN 2336–3827, online at http://sw3d.cz)

used for anisotropy of arbitrary symmetry. The WA parameters can be used for anisotropy of any strength. They are related to the used coordinate system and not to the elements of the anisotropy symmetry as Thomsen-type parameters. For more details, see Farra et al. (2015). The formulae presented and tested in this paper are based on formulae derived by Pšenčík and Vavryčuk (2002), Farra (2004) and Farra and Pšenčík (2013). They are applicable to weakly anisotropic media of arbitrary symmetry. The above references contain an important approximate relation between the *ray vector* $\mathbf{N}$ specifying the direction of the ray velocity and the *phase vector* $\mathbf{n}$, representing a normal to the wavefront (parallel to the slowness vector).

In the following section, we present three approximate expressions of increasing accuracy for the square of the P-wave ray velocity for anisotropic media of arbitrary symmetry. Afterwards, we test the accuracy of the approximate formulae on several models of different anisotropy symmetries.

Approximate ray-velocity expressions

Farra and Pšenčík (2013) offer three following possibilities for approximate computation of the square of the ray velocity in the direction of the ray vector $\mathbf{N}$. In all of them, the *first-order approximation* $\tilde{c^2}(\mathbf{N})$ of the square of the phase velocity c is used:

$$\tilde{c^2}(\mathbf{N}) = B_{33}(\mathbf{N}) \ . \tag{1}$$

Here $B_{33}(\mathbf{N})$ is an element of a matrix $\mathbf{B}$, which plays an important role in the approximate expressions describing wave propagation in weakly anisotropic media. More details about the matrix $\mathbf{B}$ and explicit expressions for its elements B_{13}, B_{23} and B_{33} are given in Appendix A.

In the derivation of the most accurate formula for the ray velocity and in numerical examples, we also use the *second-order approximation* $\tilde{\tilde{c^2}}(\mathbf{N})$ of the square of the phase velocity c

$$\tilde{\tilde{c^2}}(\mathbf{N}) = \tilde{c^2}(\mathbf{N}) + \frac{B_{13}^2(\mathbf{N}) + B_{23}^2(\mathbf{N})}{\alpha_0^2 - \beta_0^2} \ . \tag{2}$$

Here α_0 and β_0 are the reference P- and S-wave velocities. We can choose them arbitrarily, it is desirable that the corresponding WA parameters (see Appendix A) are small. Quantities B_{13} and B_{23} are again elements of the matrix $\mathbf{B}$ specified and described in Appendix A.

In the most inaccurate approximation, we ignore the difference between the vectors $\mathbf{n}$ and $\mathbf{N}$ and express the *first-order approximation* $\tilde{v^2}(\mathbf{N})$ of the square of the ray velocity v in terms of the first-order approximation of the square of the phase velocity c, see (1). In such a way, we get:

$$\tilde{v^2}(\mathbf{N}) = \tilde{c^2}(\mathbf{N}) \ . \tag{3}$$

More accurate expression is obtained if we consider the difference between the vectors $\mathbf{n}$ and $\mathbf{N}$ and express the *first-order approximation* $\tilde{v^2}(\mathbf{N})$ of the square of the ray velocity v in terms of the first-order approximation of the square of the phase velocity c, see (1). We obtain:

$$\tilde{v^2}(\mathbf{N}) = \tilde{c^2}(\mathbf{N}) - \frac{4[B_{13}^2(\mathbf{N}) + B_{23}^2(\mathbf{N})]}{\tilde{c^2}(\mathbf{N})} \ . \tag{4}$$

Most accurate formula in this paper is the *second-order approximation* $\tilde{\tilde{v}}^2(\mathbf{N})$ of the square of the ray velocity, obtained by considering the difference between vectors $\mathbf{n}$ and $\mathbf{N}$ and expressing the square of the ray velocity in terms of the second-order approximation of the square of the phase velocity c, see (2). We get:

$$\tilde{\tilde{v}}^2(\mathbf{N}) = \tilde{c}^2(\mathbf{N}) + \frac{4a[B_{13}^2(\mathbf{N}) + B_{23}^2(\mathbf{N})]}{\tilde{c}^2(\mathbf{N})} \ . \tag{5}$$

In equation (5), $a = (r^2 - 3/4)/(1 - r^2)$, where $r = \beta_0/\alpha_0$.

Tests of accuracy

Let us evaluate relative errors $(v^{appr} - v)/v \times 100\%$ of the ray velocity obtained from formulae (3), (4) and (5). Here v^{appr} is the approximate ray velocity calculated from the above formulae and v is the ray velocity calculated from the exact expression:

$$v_i(\mathbf{n}) = a_{ijkl} p_l g_j g_k \ . \tag{6}$$

In (6), a_{ijkl} are elements of the density-normalized stiffness tensor, p_i are the components of the P-wave slowness vector $\mathbf{p} = \mathbf{n}/c$ and g_i are the components of the P-wave polarization vector $\mathbf{g}$. Because approximations of the phase velocity play an important role in the evaluation of the ray velocity, we also present plots of relative errors of the first-order (1) and second-order (2) approximations of the phase velocity. The relative errors are calculated in the same way as for the ray velocities. The exact phase velocity c is obtained from the expression

$$c^2(\mathbf{n}) = a_{ijkl} n_j n_l g_i g_k \ . \tag{7}$$

The approximate phase velocities are calculated from equations (1) and (2) with the vector $\mathbf{N}$ replaced by $\mathbf{n}$.

The plots have a form of maps of isolines of the relative errors. In case of ray velocities, the plots are specified by the ray vector $\mathbf{N}$,

$$\mathbf{N} \equiv (\cos\Phi \sin\Theta,\ \sin\Phi \sin\Theta,\ \cos\Theta) \ . \tag{8}$$

In case of phase velocities, the plots are specified by the phase vector $\mathbf{n}$,

$$\mathbf{n} \equiv (\cos\phi \sin\theta,\ \sin\phi \sin\theta,\ \cos\theta) \ . \tag{9}$$

We test the formulae (3), (4) and (5) on several models with different anisotropy symmetries. Specifically, we consider models of transverse isotropy with horizontal symmetry axis (HTI), of orthorhombic symmetry (ORT), of monoclinic symmetry (MONO) and of triclinic symmetry (TRI). In all cases, we assume that the symmetry planes (axes) of the considered models coincide with coordinate planes (axes). The matrices of the density-normalized elastic moduli in the Voigt notation are given in Appendix B. In all cases the reference velocities α_0 and β_0 were chosen as $\alpha_0^2 = A_{33}$ and $\beta_0^2 = A_{44}$.

Figures 1 and 2 show maps of relative errors of ray (Figure 1) and phase (Figure 2) velocities for the model HTI, see (B1). The plots can be compared with results of other

approximate formulae for the same model, presented by Fomel (2004). The plots in Figure 1, from the top to the bottom, correspond to formulae (3), (4) and (5). The top plot shows the maximum relative error of 2.6%, which corresponds, as expected (because the formula is of the same order), to Thomsen (1986) approximation, as shown by Fomel (2004) in his Figure 4. If we take into account the difference between ray and phase vectors, and use the first-order approximation of the square of the phase velocity, i.e., if we use formula (4), the maximum relative error decreases to 1.8%, which is slightly lower value than that obtained with the approximate formula of Muir and Dellinger (1985), see again Figure 4 of Fomel (2004). One should remember that the formula of Muir and Dellinger (1985) is based on an *anelliptic* approximation, i.e., the reference medium is a medium of elliptical anisotropy while formula (4) starts from a spherical (isotropic) reference. Finally, the second-order formula (5) gives maximum error of 0.6%. It is higher than the error of Fomel's (2004) anelliptic formula, but substantially lower than all other formulae tested by Fomel (2004).

Maximum relative errors of the first-order approximation of the P-wave phase velocity in the top plot of Figure 2 reach 1.35%, which corresponds, as expected, to maximum errors of Thomsen (1986) phase-velocity formula, see Figure 3 of Fomel (2004). Use of the second-order formula (2) in the bottom plot of Figure 2 leads to a considerable reduction of relative errors by nearly an order. The accuracy of the second-order formula is comparable to to the accuracy of Fomel's (2004) anelliptic approximation.

Figures 3 and 4 show maps of relative errors of ray and phase velocities for the orthorhombic model ORT, see (B2). Because of the different symmetry, the distribution of relative errors has a different character than in the HTI model. In this case, the results can be compared with results of other formulae obtained for the same model, presented by Sripanich and Fomel (2014) and Hao and Stovas (2015). As expected, the maximum relative error of the most inaccurate formula (3) is about 2.8% and is comparable with errors of other first-order formulae presented in Figure 4 of Sripanich and Fomel (2014) and Figure 3 of Hao and Stovas (2015). There only seems to be a difference in the distribution of the errors. The maximum relative error is reduced to about 2% when the formula (4) is used. A dramatic reduction of relative errors occurs when the formula (5) is used. The maximum error of about 0.56% is comparable with the error of the formula proposed by Sripanich and Fomel (2014), see their Figure 5 or Figure 3 of Hao and Stovas (2015). Only rather complicated GMA (General Moveout Approximation) formula of the latter authors seems to yield more accurate results.

Maximum relative errors of about 1.54% of the first-order P-wave phase-velocity approximation shown in the top plot of Figure 4 are again comparable with errors of other first-order formulae tested by Sripanich and Fomel (2014) and Hao and Stovas (2015). The second-order phase velocity approximation reduces the maximum error to about 0.16%, which is less than the errors of the formula proposed by Sripanich and Fomel (2014). It is, however, higher than the errors of the GMA formula of Hao and Stovas (2015).

Figures 5 and 6 show maps of relative errors of ray and phase velocities for the monoclinic model MONO, see (B3) and Figures 7 and 8 for the triclinic model TRI, see (B4). Due to different symmetries, the character of the distribution of relative errors of formulae (3)-(5) is different, but maximum relative errors are, approximately of the same order as in the two previous models.

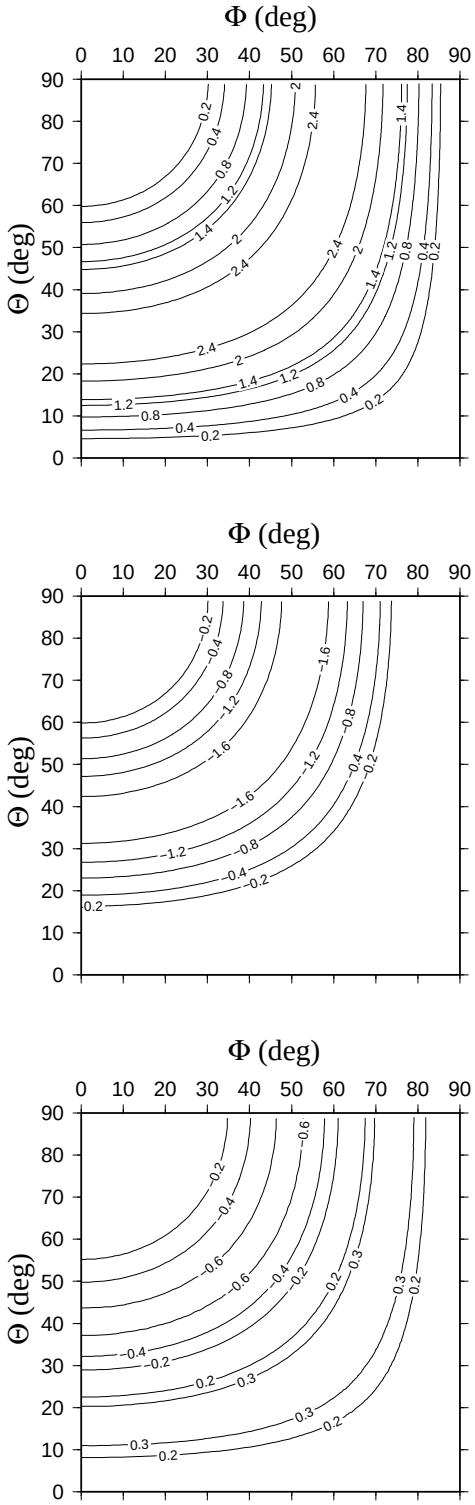

Figure 1: HTI model. Maps of relative errors of the approximate ray-velocity formulae (3), top, (4), middle, and (5), bottom. Θ and Φ are polar and azimuthal angles specifying the direction of the ray vector, see (8).

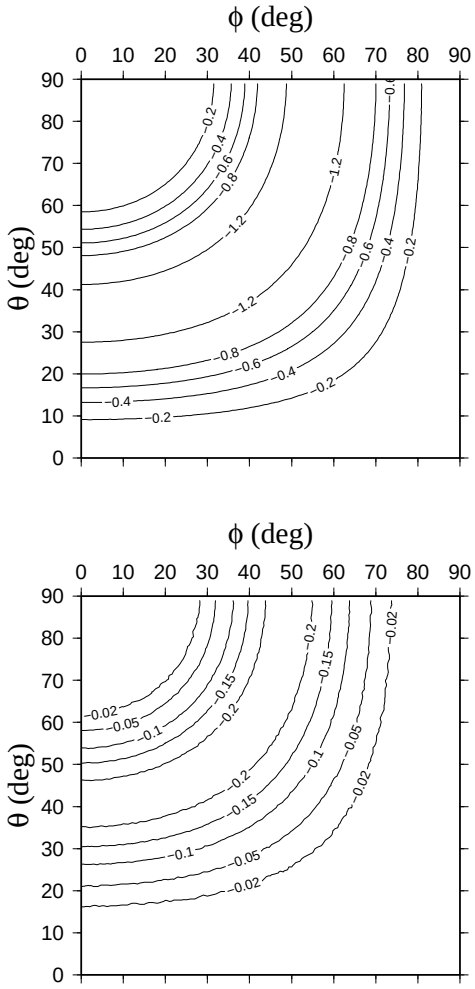

Figure 2: HTI model. Maps of relative errors of the first- (top) and second-order phase-velocity formulae (1) and (2), respectively. θ and ϕ are polar and azimuthal angles specifying the direction of the phase vector, see (9).

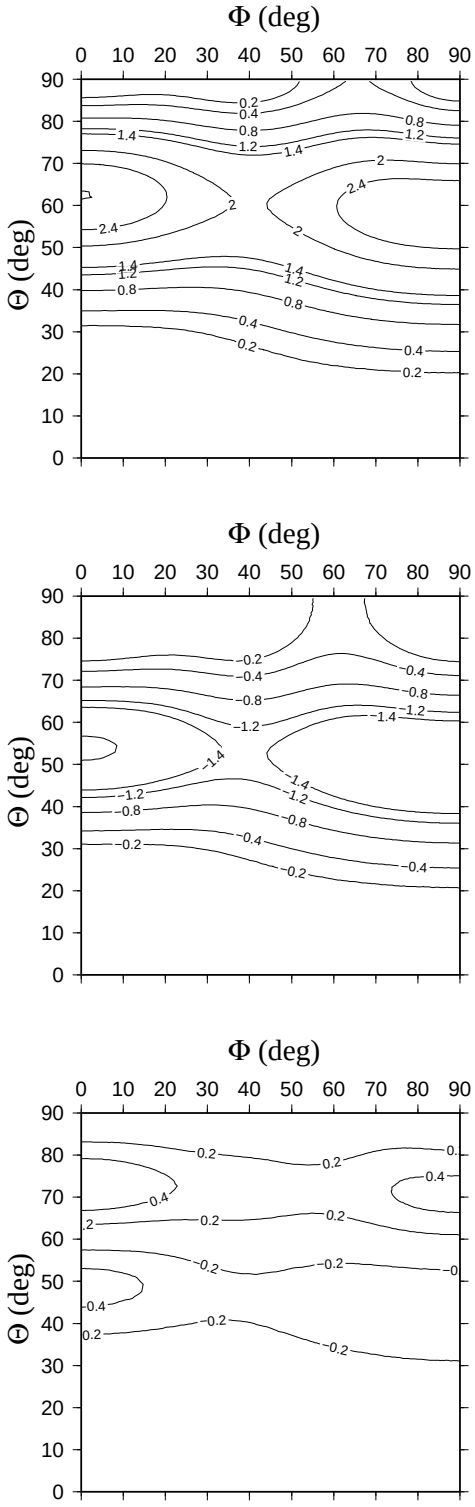

Figure 3: ORT model. Maps of relative errors of the approximate ray-velocity formulae (3), top, (4), middle, and (5), bottom. Θ and Φ are polar and azimuthal angles specifying the direction of the ray vector, see (8).

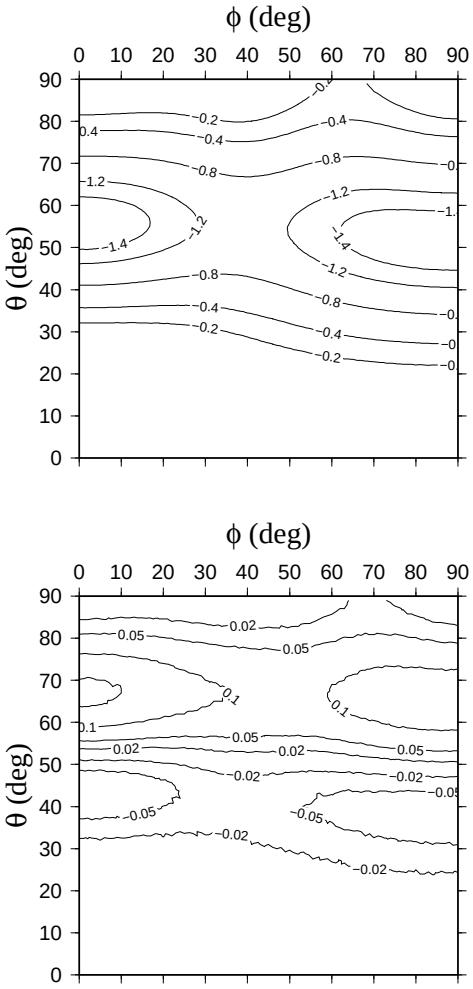

Figure 4: ORT model. Maps of relative errors of the first- (top) and second-order phase-velocity formulae (1) and (2), respectively. θ and ϕ are polar and azimuthal angles specifying the direction of the phase vector, see (9).

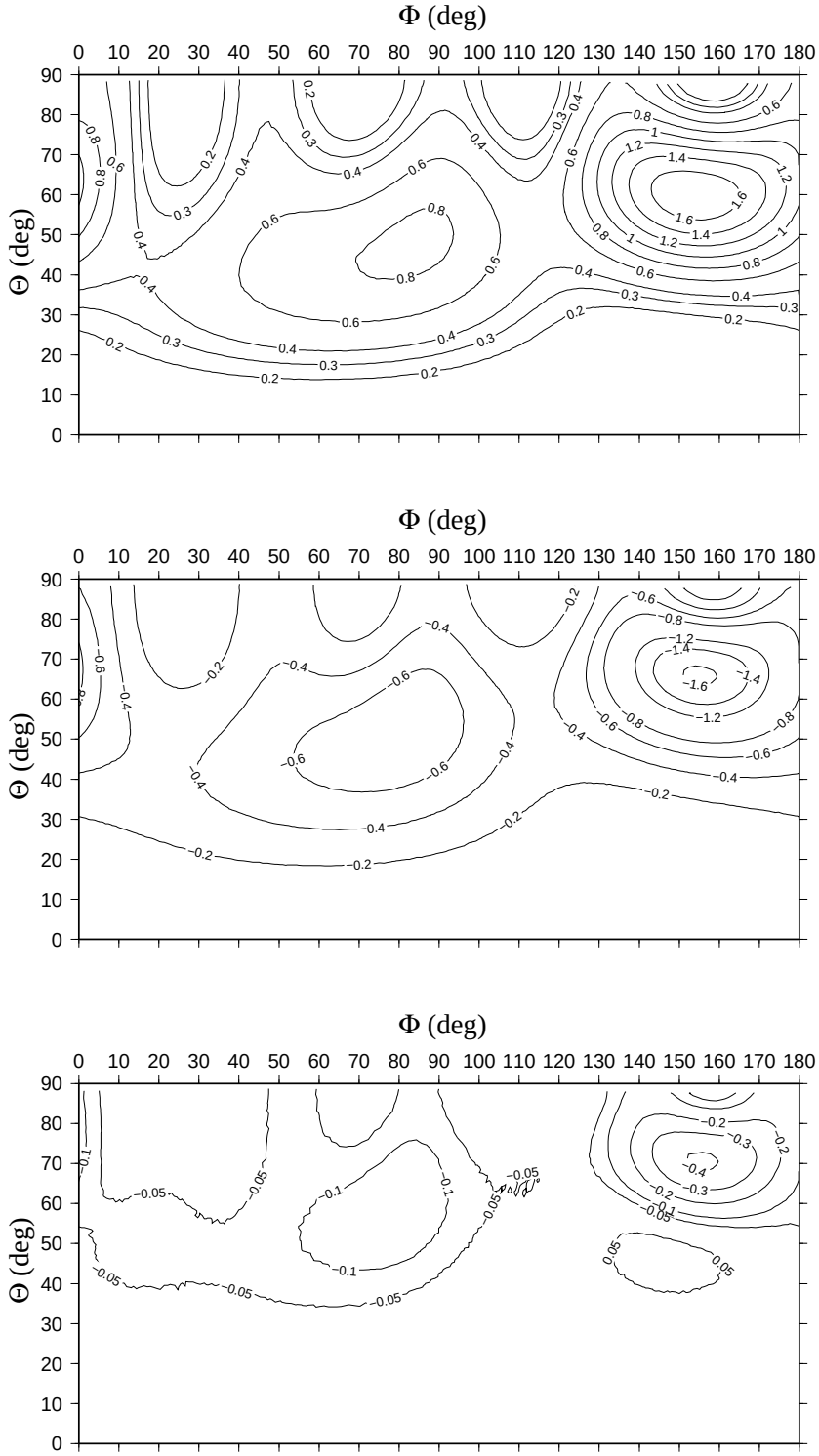

Figure 5: MONO model. Maps of relative errors of the approximate ray-velocity formulae (3), top, (4), middle, and (5), bottom. Θ and Φ are polar and azimuthal angles specifying the direction of the ray vector, see (8).

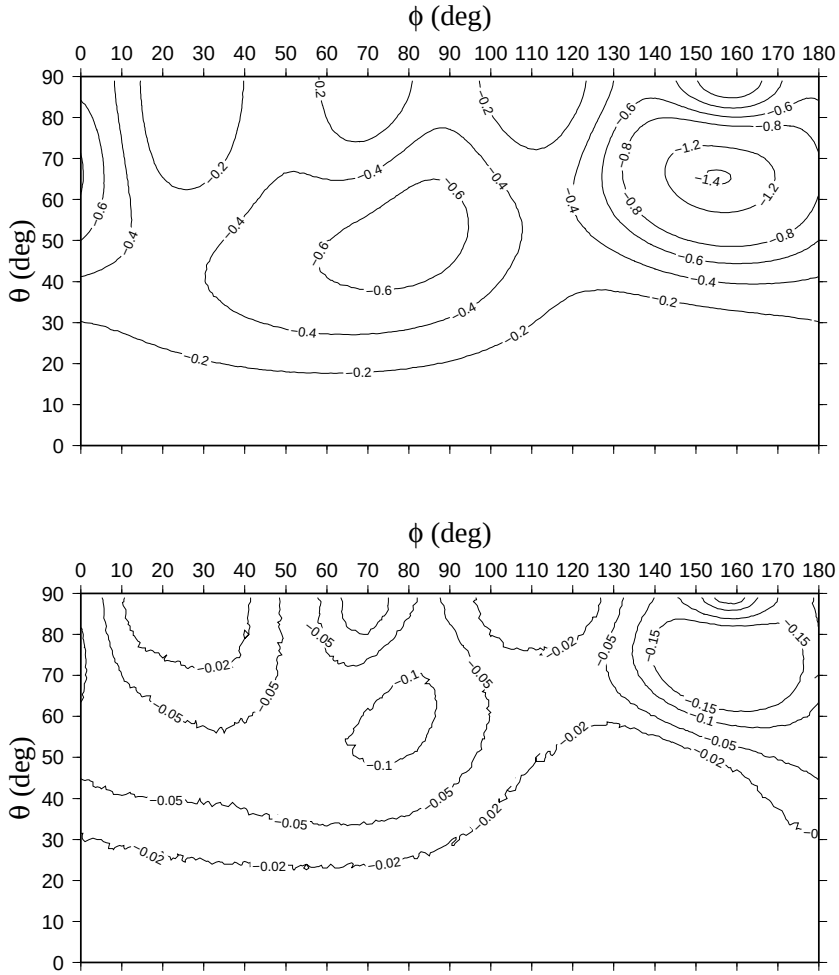

Figure 6: MONO model. Maps of relative errors of the first- (top) and second-order phase-velocity formulae (1) and (2), respectively. θ and ϕ are polar and azimuthal angles specifying the direction of the phase vector, see (9).

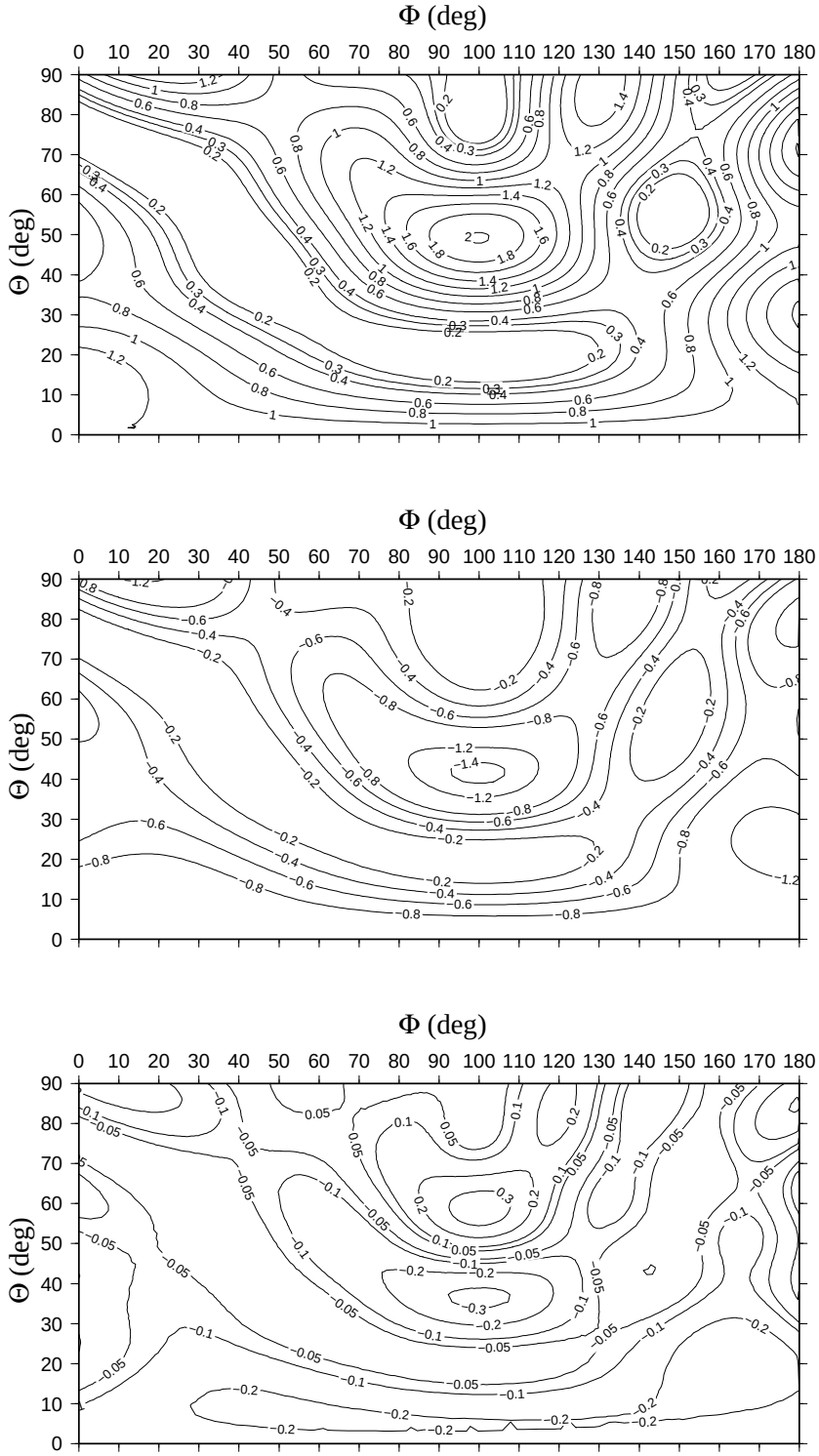

Figure 7: TRI model. Maps of relative errors of the approximate ray-velocity formulae (3), top, (4), middle, and (5), bottom. Θ and Φ are polar and azimuthal angles specifying the direction of the ray vector, see (8).

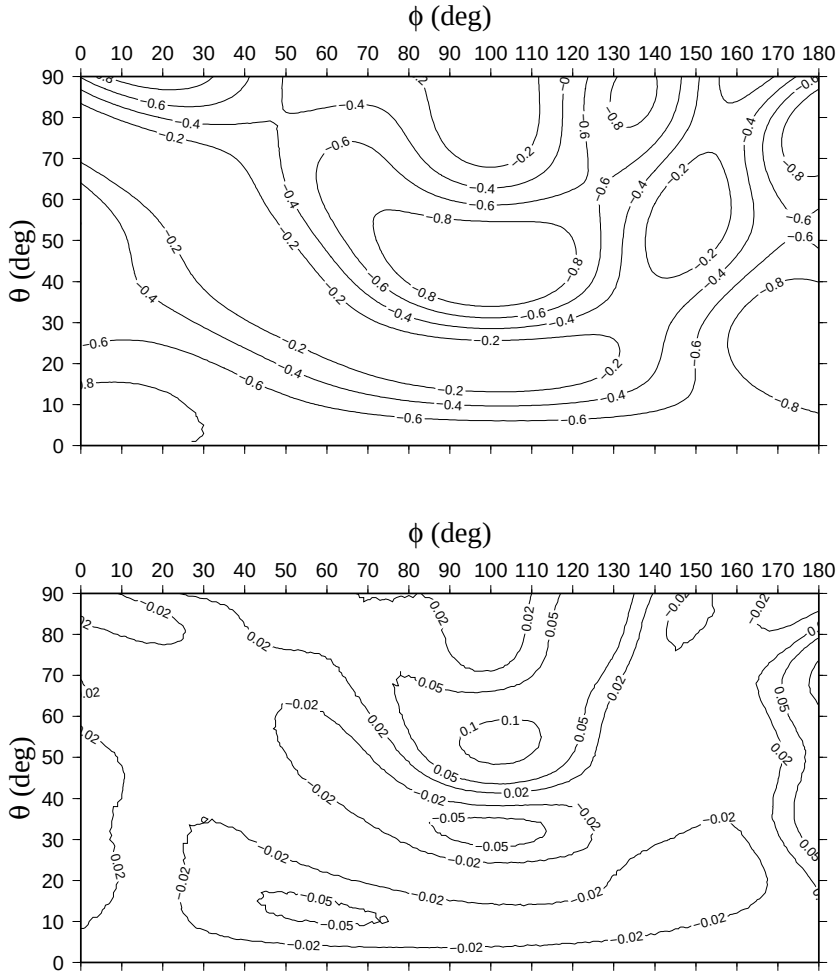

Figure 8: TRI model. Maps of relative errors of the first- (top) and second-order phase-velocity formulae (1) and (2), respectively. θ and ϕ are polar and azimuthal angles specifying the direction of the phase vector, see (9).

Conclusions

We test accuracy of the approximate P-wave ray-velocity (and as a by-product also phase-velocity) formulae of varying accuracy, based on weak-anisotropy approximation. While the phase-velocity formulae are specified in a standard way by the phase vector (vector parallel to the slowness vector), the ray-velocity formulae are specified by the ray vector (vector parallel to the ray velocity vector). The accuracy of the formulae depends on two factors: if we consider or do not consider the difference between the ray and phase vectors and if we use the first- or second-order approximation of the square of the phase velocity.

The used formulae are based only on the assumption of weak anisotropy. No non-physical assumptions like zero S-wave phase velocities (Alkhalifah, 2000a, 2003) are used.

Comparisons show that especially the approximation based on the second-order phase velocity and taking into account the difference between the phase and ray vectors yields results of accuracy comparable with formulae based on the so-called anelliptic approximation (approximation, which is based on perturbations from a reference medium of elliptical anisotropy; formulae presented in this paper are based on perturbations of a reference isotropic medium). It is also necessary to emphasize that anisotropy of several of the tested models cannot be considered weak. This means that the presented formulae work with sufficient accuracy even in moderately anisotropic media.

Weak-anisotropy parameters are used for the parameterization of the medium in all used formulae. This parameterization is universal and can be used for any anisotropic symmetry including such as monoclinic and triclinic. This is different from the commonly used procedures, in which a different parameterization is used for each anisotropy symmetry. The parameterization by WA parameters can even be used for the specification of other seismic attributes as, for example, polarization vectors.

The expressions for the squares of ray velocity are relatively simple. They, for example, contain no square roots. The first-order expressions for the ray velocity (3) and (4) are independent of the choice of the reference isotropic medium (specified by α_0 and β_0). The second-order expression (5) depends only weakly on the ratio of β_0 and α_0. The presented formulae for squares of both ray and phase velocities are expressed in terms of three elements B_{13}, B_{23} and B_{33} of the matrix $\mathbf{B}$. The matrix $\mathbf{B}$ represents a result of the rotation of the Christoffel matrix into the coordinate frame related to a ray. Each of the referred elements is a linear function of WA parameters. The number of WA parameters varies with the considered symmetry. It is 15, 9, 6 and 3 for triclinic, monoclinic, orthorhombic and TI symmetry. These numbers can be further reduced by one if the square of the reference P-wave velocity α_0^2 used in the formulae is specified as $\alpha_0^2 = A_{33}$.

Appendix A: WA parameters and matrix B

Let us consider a Cartesian coordinate system with the x_3-axis vertical, positive downwards. The elements B_{mn} of matrix $\mathbf{B}$ used in the approximate expressions for the phase and ray velocities are given by the formula:

$$B_{mn}(\mathbf{n}) = a_{ijkl} n_j n_l e_i^{[m]} e_k^{[n]}. \qquad (A1)$$

Here a_{ijkl} are density-normalized elastic moduli (elements of the stiffness tensor). Symbols n_i denote components of a unit vector $\mathbf{n}$. Unit, mutually perpendicular vectors $\mathbf{e}^{[i]}$ are defined in the following way:

$$\mathbf{e}^{[1]} \equiv D^{-1}(n_1 n_3, n_2 n_3, n_3^2 - 1), \quad \mathbf{e}^{[2]} \equiv D^{-1}(-n_2, n_1, 0), \quad \mathbf{e}^{[3]} = \mathbf{n} \equiv (n_1, n_2, n_3), \quad (A2)$$

where

$$D = (n_1^2 + n_2^2)^{1/2}, \quad n_1^2 + n_2^2 + n_3^2 = 1. \qquad (A3)$$

Matrix $\mathbf{B}$ in (A1) is Christoffel matrix rotated to the Cartesian coordinate system whose basis vectors are vectors $\mathbf{e}^{[i]}$.

Explicit expressions for elements of matrix $\mathbf{B}$ for an anisotropic medium of arbitrary symmetry and strength in terms of 21 weak-anisotropy (WA) parameters were introduced by Farra and Pšenčík (2003). P-wave attributes depend on three elements of matrix $\mathbf{B}$, specifically, B_{13}, B_{23} and B_{33}. Matrix $\mathbf{B}$ and, therefore, also the referred elements, are independent of the reference velocity α_0. In addition, the terms B_{33} and $B_{13}^2 + B_{23}^2$ are independent of the choice of the vectors $\mathbf{e}^{[1]}$ and $\mathbf{e}^{[2]}$ in the plane perpendicular to $\mathbf{n}$. Each of the above three elements depends on 15 (P-wave) WA parameters in the case of most general anisotropy. Element $B_{33}(\mathbf{n})$ represents the first-order approximation $\tilde{c}^2(\mathbf{n})$ of the square of the phase velocity. For the specification (A2), (A3), the elements B_{13}, B_{23} and B_{33} read:

$$\begin{aligned}
B_{13}(\mathbf{n}) = \alpha_0^2 D^{-1}\{ & n_3^4(\epsilon_{34} n_2 + \epsilon_{35} n_1) + n_3^3[(\delta_y - \epsilon_x - \epsilon_z) n_1^2 + (\delta_x - \epsilon_y - \epsilon_z) n_2^2 + 2\chi_z n_1 n_2] \\
& + n_3^2[(4\chi_x - 3\epsilon_{34}) n_1^2 n_2 + (4\chi_y - 3\epsilon_{35}) n_1 n_2^2 + (4\epsilon_{15} - 3\epsilon_{35}) n_1^3 + (4\epsilon_{24} - 3\epsilon_{34}) n_2^3] \\
& + n_3[(2\delta_z - \delta_y - \delta_x - \epsilon_x - \epsilon_y + 2\epsilon_z) n_1^2 n_2^2 + 2(2\epsilon_{16} - \chi_z) n_1^3 n_2 + 2(2\epsilon_{26} - \chi_z) n_1 n_2^3 \\
& + (\epsilon_x + \epsilon_z - \delta_y) n_1^4 + (\epsilon_y + \epsilon_z - \delta_x) n_2^4 + (\epsilon_x - \epsilon_z) n_1^2 + (\epsilon_y - \epsilon_z) n_2^2] \\
& - \chi_x n_1^2 n_2 - \chi_y n_1 n_2^2 - \epsilon_{15} n_1^3 - \epsilon_{24} n_2^3\},
\end{aligned}$$

$$\begin{aligned}
B_{23}(\mathbf{n}) = \alpha_0^2 D^{-1}\{ & n_3^3(\epsilon_{34} n_1 - \epsilon_{35} n_2) + n_3^2[(\delta_x - \delta_y - \epsilon_y + \epsilon_x) n_1 n_2 + \chi_z n_1^2 - \chi_z n_2^2] \\
& + n_3[(2\chi_y - 3\epsilon_{15}) n_1^2 n_2 - (2\chi_x - 3\epsilon_{24}) n_1 n_2^2 + \chi_x n_1^3 - \chi_y n_2^3] \\
& + (\delta_z - \epsilon_x - \epsilon_y) n_1^3 n_2 - (\delta_z - \epsilon_x - \epsilon_y) n_1 n_2^3 + 3(\epsilon_{26} - \epsilon_{16}) n_1^2 n_2^2 + \epsilon_{16} n_1^4 - \epsilon_{26} n_2^4 + (\epsilon_y - \epsilon_x) n_1 n_2\},
\end{aligned}$$

$$B_{33}(\mathbf{n}) = \alpha_0^2\{1 + 4n_3^3(\epsilon_{34} n_2 + \epsilon_{35} n_1) + 2n_3^2[(\delta_y - \epsilon_x - \epsilon_z) n_1^2 + (\delta_x - \epsilon_y - \epsilon_z) n_2^2 + 2\chi_z n_1 n_2 + \epsilon_z]$$

$$+4n_3(\chi_x n_1^2 n_2+\chi_y n_1 n_2^2+\epsilon_{15} n_1^3+\epsilon_{24} n_2^3)+2\epsilon_x n_1^2+2\epsilon_y n_2^2+2(\delta_z-\epsilon_x-\epsilon_y)n_1^2 n_2^2+4\epsilon_{16} n_1^3 n_2+4\epsilon_{26} n_1 n_2^3\}. \tag{A4}$$

The WA parameters used in (A4) are defined as

$$\epsilon_x = \frac{A_{11}-\alpha_0^2}{2\alpha_0^2}\ , \quad \epsilon_y = \frac{A_{22}-\alpha_0^2}{2\alpha_0^2}\ , \quad \epsilon_z = \frac{A_{33}-\alpha_0^2}{2\alpha_0^2}\ ,$$

$$\delta_x = \frac{A_{23}+2A_{44}-\alpha_0^2}{\alpha_0^2}\ , \quad \delta_y = \frac{A_{13}+2A_{55}-\alpha_0^2}{\alpha_0^2}\ , \quad \delta_z = \frac{A_{12}+2A_{66}-\alpha_0^2}{\alpha_0^2}\ ,$$

$$\chi_x = \frac{A_{14}+2A_{56}}{\alpha_0^2}\ , \quad \chi_y = \frac{A_{25}+2A_{46}}{\alpha_0^2}\ , \quad \chi_z = \frac{A_{36}+2A_{45}}{\alpha_0^2}\ ,$$

$$\epsilon_{15} = \frac{A_{15}}{\alpha_0^2}\ , \quad \epsilon_{16} = \frac{A_{16}}{\alpha_0^2}\ , \quad \epsilon_{24} = \frac{A_{24}}{\alpha_0^2}\ , \quad \epsilon_{26} = \frac{A_{26}}{\alpha_0^2}\ , \quad \epsilon_{34} = \frac{A_{34}}{\alpha_0^2}\ , \quad \epsilon_{35} = \frac{A_{35}}{\alpha_0^2}\ . \tag{A5}$$

The symbols $A_{\alpha\beta}$ are the density-normalized elastic moduli a_{ijkl} in the Voigt notation. The symbol α_0 in (A4) and (A5) denotes the P-wave velocity in a reference (background) isotropic medium.

In a monoclinic medium whose plane of symmetry coincides with the plane (x_1, x_2), the number of WA parameters specifying P-wave propagation reduces to 9 because

$$\epsilon_{15} = \epsilon_{24} = \epsilon_{34} = \epsilon_{35} = \chi_x = \chi_y = 0\ . \tag{A6}$$

The elements B_{13}, B_{23} and B_{33} of matrix $\mathbf{B}$ attain the following form:

$$B_{13}(\mathbf{n}) = \alpha_0^2 D^{-1}\{n_3^3[(\delta_y-\epsilon_x-\epsilon_z)n_1^2+(\delta_x-\epsilon_y-\epsilon_z)n_2^2+2\chi_z n_1 n_2]$$

$$+n_3[(2\delta_z-\delta_y-\delta_x-\epsilon_x-\epsilon_y+2\epsilon_z)n_1^2 n_2^2+2(2\epsilon_{16}-\chi_z)n_1^3 n_2+2(2\epsilon_{26}-\chi_z)n_1 n_2^3$$
$$+(\epsilon_x+\epsilon_z-\delta_y)n_1^4+(\epsilon_y+\epsilon_z-\delta_x)n_2^4+(\epsilon_x-\epsilon_z)n_1^2+(\epsilon_y-\epsilon_z)n_2^2]\},$$

$$B_{23}(\mathbf{n}) = \alpha_0^2 D^{-1}\{n_3^2[(\delta_x-\delta_y-\epsilon_y+\epsilon_x)n_1 n_2+\chi_z n_1^2-\chi_z n_2^2]$$
$$+(\delta_z-\epsilon_x-\epsilon_y)n_1^3 n_2-(\delta_z-\epsilon_x-\epsilon_y)n_1 n_2^3+3(\epsilon_{26}-\epsilon_{16})n_1^2 n_2^2+\epsilon_{16}n_1^4-\epsilon_{26}n_2^4+(\epsilon_y-\epsilon_x)n_1 n_2\},$$

$$B_{33}(\mathbf{n}) = \alpha_0^2\{1+2n_3^2[(\delta_y-\epsilon_x-\epsilon_z)n_1^2+(\delta_x-\epsilon_y-\epsilon_z)n_2^2+2\chi_z n_1 n_2+\epsilon_z]$$
$$+2\epsilon_x n_1^2+2\epsilon_y n_2^2+2(\delta_z-\epsilon_x-\epsilon_y)n_1^2 n_2^2+4\epsilon_{16}n_1^3 n_2+4\epsilon_{26}n_1 n_2^3\}. \tag{A7}$$

In an orthorhombic medium whose planes of symmetry coincide with coordinate planes, the number of WA parameters specifying P-wave propagation reduces to 6 because

$$\epsilon_{16} = \epsilon_{26} = \chi_z = 0\ . \tag{A8}$$

The elements B_{13}, B_{23} and B_{33} attain the following form:

$$B_{13}(\mathbf{n}) = \alpha_0^2 D^{-1}\{n_3^3[(\delta_y-\epsilon_x-\epsilon_z)n_1^2+(\delta_x-\epsilon_y-\epsilon_z)n_2^2]$$

$$+n_3[(2\delta_z-\delta_y-\delta_x-\epsilon_x-\epsilon_y+2\epsilon_z)n_1^2 n_2^2$$

$$+(\epsilon_x+\epsilon_z-\delta_y)n_1^4+(\epsilon_y+\epsilon_z-\delta_x)n_2^4+(\epsilon_x-\epsilon_z)n_1^2+(\epsilon_y-\epsilon_z)n_2^2]\},$$

$$B_{23}(\mathbf{n})=\alpha_0^2D^{-1}[(\delta_x-\delta_y-\epsilon_y+\epsilon_x)n_1n_2n_3^2$$
$$+(\delta_z-\epsilon_x-\epsilon_y)n_1^3n_2-(\delta_z-\epsilon_x-\epsilon_y)n_1n_2^3+(\epsilon_y-\epsilon_x)n_1n_2],$$

$$B_{33}(\mathbf{n})=\alpha_0^2\{1+2n_3^2[(\delta_y-\epsilon_x-\epsilon_z)n_1^2+(\delta_x-\epsilon_y-\epsilon_z)n_2^2+\epsilon_z]$$
$$+2\epsilon_xn_1^2+2\epsilon_yn_2^2+2(\delta_z-\epsilon_x-\epsilon_y)n_1^2n_2^2\}. \qquad (A9)$$

In a transversely isotropic medium with axis of symmetry coinciding with one of the coordinate lines, the number of WA parameters specifying P-wave propagation reduces to 3. In an HTI medium with axis of symmetry parallel to the x_1 axis the WA parameters satisfy the following additional conditions:

$$\epsilon_y=\epsilon_z=\frac{1}{2}\delta_x\ ,\delta_y=\delta_z\ . \qquad (A10)$$

The elements B_{13}, B_{23} and B_{33} attain the following form:

$$B_{13}(\mathbf{n})=\alpha_0^2D^{-1}\{(\delta_y-\epsilon_x-\epsilon_y)n_1^2n_3^3+n_3[(\epsilon_x+\epsilon_y-\delta_y)n_1^4+(\epsilon_x-\epsilon_y)n_1^2]\},$$

$$B_{23}(\mathbf{n})=\alpha_0^2D^{-1}[(\epsilon_y+\epsilon_x-\delta_y)n_1n_2n_3^2$$
$$+(\delta_y-\epsilon_x-\epsilon_y)n_1^3n_2-(\delta_y-\epsilon_x-\epsilon_y)n_1n_2^3+(\epsilon_y-\epsilon_x)n_1n_2],$$

$$B_{33}(\mathbf{n})=\alpha_0^2\{1+2n_3^2[(\delta_y-\epsilon_x-\epsilon_y)n_1^2+\epsilon_y]$$
$$+2\epsilon_xn_1^2+2\epsilon_yn_2^2+2(\delta_y-\epsilon_x-\epsilon_y)n_1^2n_2^2\}. \qquad (A11)$$

Appendix B: Matrices of elastic moduli of tested models

As a model of transversely isotropic medium we consider the Greenhorn shale of Fomel (2004) with the axis of symmetry coinciding with the coordinate x_1-axis. The density-normalized elastic moduli of the HTI model (with artificially completed the lower right part) in $(\mathrm{km/s})^2$ are:

$$\begin{pmatrix} 9.57283 & 4.51203 & 4.51203 & 0 & 0 & 0 \\ & 14.47413 & 9.91393 & 0 & 0 & 0 \\ & & 14.47413 & 0 & 0 & 0 \\ & & & 2.28010 & 0 & 0 \\ & & & & 2.28010 & 0 \\ & & & & & 2.28010 \end{pmatrix} \qquad (B1)$$

As an orthorhombic model, ORT, we use the model proposed by Schoenberg and Helbig (1997). The density-normalized elastic moduli of this model in $(\mathrm{km/s})^2$ are:

$$\begin{pmatrix} 9.00 & 3.60 & 2.25 & 0 & 0 & 0 \\ & 9.84 & 2.40 & 0 & 0 & 0 \\ & & 5.9375 & 0 & 0 & 0 \\ & & & 2.00 & 0 & 0 \\ & & & & 1.60 & 0 \\ & & & & & 2.182 \end{pmatrix} \qquad (B2)$$

As a monoclinic model, MONO, we use the model used by Farra et al. (2015), with the density-normalized elastic moduli in $(\mathrm{km/s})^2$:

$$\begin{pmatrix} 4.952 & 0.433 & 0.625 & 0 & 0 & 0.385 \\ & 5.096 & 1.010 & 0 & 0 & -0.288 \\ & & 6.779 & 0 & 0 & -0.481 \\ & & & 2.452 & 0 & 0 \\ & & & & 2.885 & 0 \\ & & & & & 2.356 \end{pmatrix} \qquad (B3)$$

As a triclinic model, TRI, we use the model used by Grechka (2015), with the density-normalized elastic moduli in $(\mathrm{km/s})^2$:

$$\begin{pmatrix} 19.81 & 8.62 & 9.00 & -2.37 & -1.44 & 0.95 \\ & 25.79 & 9.09 & 0.57 & -0.99 & -0.89 \\ & & 20.68 & -2.10 & 0.43 & 0.49 \\ & & & 7.17 & -0.15 & -0.08 \\ & & & & 8.14 & -0.33 \\ & & & & & 6.49 \end{pmatrix} \qquad (B4)$$

References

Alkhalifah, T., 2000a. An acoustic wave equation for anisotropic media. *Geophysics*, **65**, 1239–1250.

Alkhalifah, T., 2000b. The offset-midpoint traveltime pyramide for transversely isotropic media. *Geophysics*, **65**, 1316–1325.

Alkhalifah, T., 2003. An acoustic wave equation for orthorhombic anisotropy. *Geophysic*, **68**, 1169-1172.

Daley, P.F., and E.S. Krebes, 2004. Approximate QL phase and group velocities in weakly orthorhombic anisotropic media. *CREWES Research Report*, **16**.

Farra, V., 2004. Improved first-order approximation of group velocities in weakly anisotropic media. Stud. Geophys. Geod., **48**, 199–213.

Farra, V., and I. Pšenčík, 2003. Properties of the zero-, first- and higher-order approximations of attributes of elastic waves in weakly anisotropic media. *J. Acoust. Soc. Am.*, **114**, 1366–1378.

Farra, V., and I. Pšenčík, 2013. Moveout approximations for P and SV waves in VTI media. *Geophysics*, **78**, WC81–WC92.

Farra, V., I. Pšenčík, and P. Jílek, 2015. Weak-anisotropy moveout approximations for P waves in homogeneous layers of monoclinic or higher anisotropy symmetries. *Seismic Waves in Complex 3-D Structures*, **25**, 51–88, online at "http://sw3d.cz".

Fomel, S., 2004. On anelliptic approximations for qP velocities in VTI media. *Geophys. Prosp.*, **52**, 247–259.

Grechka, V., 2015. Shear-wave group-velocity surfaces in low-symmetry anisotropic media.*Geophysics*, **80**, C1-C7.

Hao, Q. and A. Stovas, 2015. Anelliptic approximation for phase and group velocities of P-waves in orthorhombic media. *Geophysics*, submitted.

Muir F., and J. Dellinger, 1985. A practical anisotropic system. *SEP 44*, 55-58. Stanford Exploration Project.

Pšenčík, I. and V. Vavryčuk, 2002. Approximate relation between the ray vector and wave normal directions in weakly anisotropic media. *Stud. geophys. geod.*, **46**, 793-807.

Schoenberg, M. and K. Helbig, 1997. Orthorhombic media: Modeling elastic wave behavior in a vertically fractured earth. *Geophysics*, **62**, 1954–1974.

Song, L-P., and A.G. Every, 2000. Approximate formulae for acoustic wave group slowness in weakly orthorhombic media. *Journal of Physics D: Applied Physics*, **33**, L81–L85.

Sripanich, Y., and S. Fomel, 2014. Anelliptic approximations for qP velocities in TI and orthorhombic media. 84th SEG annual meeting, Denver, *Extended Abstract*, 453–457.

Thomsen, L., 1986. Weak elastic anisotropy. *Geophysics*, **51**, 1954–1966.

Tsvankin, I., 2001. Seismic signatures and analysis of reflection data in anisotropic media: Oxford, Elsevier Science Ltd.

Tsvankin, I., and V. Grechka, 2011. Seismology of azimuthally anisotropic media and seismic fracture characterization. Geophysical References Series No. 17, K. Larner, M. Slawinski, volume editors, S. Fomel, managing editor. Society of Exploration Geophysicists, Tulsa.